

# **An interferometric solution for raypath-consistent shear wave statics**

Raul Cova, David Henley and Kris Innanen

## **ABSTRACT**

Converted-wave data processing requires the computation of shear-wave statics for the receiver side. Conventionally this is done under the assumption of surface consistency. However, if the velocity change between the low velocity layer (LVL) and the medium underneath is smooth, the vertical raypath assumption that supports the surface consistent approach is no longer valid. This feature results in a non-stationary change of the statics that needs to be addressed in order to properly solve the problem. In this paper the radial-trace (R-T) transform is used for moving the data to a raypath consistent framework where the statics change was showed to be approximately stationary. In this domain traveltimes interferometry was applied to retrieve the delays caused by the near surface. Cross-correlation of the delayed traces with a model trace free of statics was showed to return a cross-correlation function that carries the statics information. These functions were convolved with the original traces to remove the delay caused by the near surface. Since all the operations are done in the R-T domain an inverse radial trace transform was applied to return the data to the space-time domain. Stacked sections computed using surface- and raypath-consistent solutions showed how the latter one effectively removed the statics by addressing the non-stationarity of the problem. The analysis of the trend of the cross-correlation functions for different receiver locations showed that there is a link between the delays captured by these functions in the R-T domain and the traveltimes through the near surface at different raypath angles. Such information could be used in an inversion algorithm to retrieve a velocity model for the near surface.

## **INTRODUCTION**

Computation of receiver statics when processing converted-wave seismic data is still an important concern in this field. Since converted-wave energy travels back to the surface with slow velocities in the form of shear-waves, the effect of the near surface on the traveltimes is several times larger than that for P-waves. This also implies that some of the simplifications made for solving P-wave statics can not be overlooked when computing S-wave statics. Cova et al. (2013) explain how raypath angle dependency is an important feature that may impose a non-stationary character to S-wave statics.

Several methods have been developed for solving S-wave statics under the surface-consistent assumption. Schafer (1991) shows a comparison of methods like hand-picking, time-difference, extended generalized Gauss-Seidel refraction, and Monte Carlo simulated annealing for computing S-wave statics. All these methods rely on the picking of S-wave refractions or PS-wave reflections which may be hard to identify at the early stages of the processing and which are very time consuming. In the last ten years, near surface characterization by inversion of ground roll dispersion has gained attention. Dulaijan (2008) used the multi-spectral analysis of surface waves (MASW) to build near surface S-wave velocity models and compute statics. However, the MASW may lack sufficient resolution

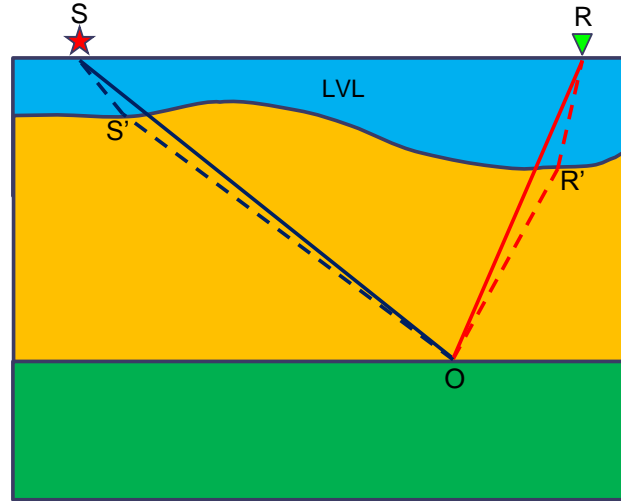


FIG. 1. Sketch showing the geometry of the static problem. Dashed paths represent a PS reflection affected by the LVL. The continuous path depicts the PS reflection we should get if there were no LVL.

when strong lateral variations of S-wave velocities are present (Lin and Lin, 2007) or when the near surface is not horizontally layered (Bodet et al., 2005).

Henley (2012) introduced an alternative approach based on the concepts of interferometry and raypath consistency. Applications of this approach has been demonstrated to be successful both for P- and S-wave statics. In this work we will show the robustness of the "raypath interferometry" for solving S-wave statics focused on the analysis of the non-stationarity of the problem. Finite difference modelling will be used for computing synthetic data and the work-flow proposed by Henley and Daley (2008) will be applied.

### Traveltime interferometry

Figure 1 depicts the geometry of the problem that needs to be solved. The dashed line represents the original raypath of a converted-wave reflection from the surface to the conversion point O. The paths SS' and RR' represent the distances traveled in the near surface both at the source and the receiver location, respectively. On the other hand, the continuous line SOR represents the traveltime we would get if there were no near surface effects. The static time we need to remove from the traveltime is given by the difference between the dashed and the continuous line and can be defined as:

$$\Delta t = \tau'_{SOR} - \tau_{SOR}. \quad (1)$$

Here,  $\tau'$  indicates the traveltime affected by the near surface and  $\tau$  represents the static-free traveltime.

Assuming that source statics have been corrected, we just keep the terms related to the raypaths on the receiver side. In that case the receiver static correction can be computed as:

$$\Delta t_R = \tau'_{OR} - \tau_{OR}. \quad (2)$$

The traveltimes subtraction in equation 2 can be retrieved by cross-correlating a static-free trace with a delayed trace. In order to show this, let us assume two spike functions  $s(t)$  and  $s'(t)$ , the first one located at the static-free time  $\tau$  and the last one at the time  $\tau'$  delayed by the static  $\Delta t_R$ ,

$$s(t) = \delta(t - \tau) \tag{3}$$

$$s'(t) = \delta(t - (\tau + \Delta t)) \tag{4}$$

Cross-correlation of both signals in the frequency domain can be written as:

$$s(t) \otimes s'(t) = F^{-1}(2\pi S(\omega)S'^*(\omega)) \tag{5}$$

where  $F^{-1}$  is the inverse Fourier transform,  $S(\omega)$  is the Fourier transform of  $s(t)$  and  $S'^*(\omega)$  is the complex conjugate of the Fourier transform of  $s'(t)$ . The Fourier transform of the delta functions are known to be exponential functions of the form of  $e^{i\omega\tau}$ . Therefore the product  $S(\omega)S'^*(\omega)$  can be written as,

$$\begin{aligned} S(\omega)S'^*(\omega) &= e^{i\omega\tau} e^{-i\omega(\tau+\Delta t)}, \\ &= e^{-i\omega\Delta t}. \end{aligned} \tag{6}$$

Substituting equation 6 into equation 5 we get,

$$\begin{aligned} s(t) \otimes s'(t) &= F^{-1}(2\pi e^{-i\omega\Delta t}), \\ &= \delta(t + \Delta t). \end{aligned} \tag{7}$$

Equation 7 shows how the cross-correlation of the static-free trace and the delayed data retrieves the traveltimes correction needed to remove the static effect from the data.

Following a similar procedure as above it can be shown that the convolution of the result in equation 7 with the delayed signal returns the static-free trace. The process of retrieving traveltimes through the use of cross-correlation functions is known as traveltimes interferometry.

### *Finite-difference modelling*

Figure 2 shows the P- and S-wave velocity models used for computing the synthetic data used in this work. The initial tests were performed on this very simple model of two flat horizons and a structurally complex LVL. No changes in P-wave velocity were included in the LVL in order to avoid P-wave statics. However, for the S-wave model the velocity of the LVL was set at 500 m/s and the medium underneath at 700 m/s. According to Snell's law this velocity contrast may allow deviations of up to 45° respect to the normal at the base of the LVL. This deviation may be enhanced for the dip at the base of the LVL posing a raypath dependency on the static solution. The reader is referred to Cova et al. (2013) for a detailed explanation of the raypath dependency observed on these data.

In Figure 3 is shown a raw radial component shot-gather with the most important events identified on the record. There we can see how the delays caused by the near surface deform

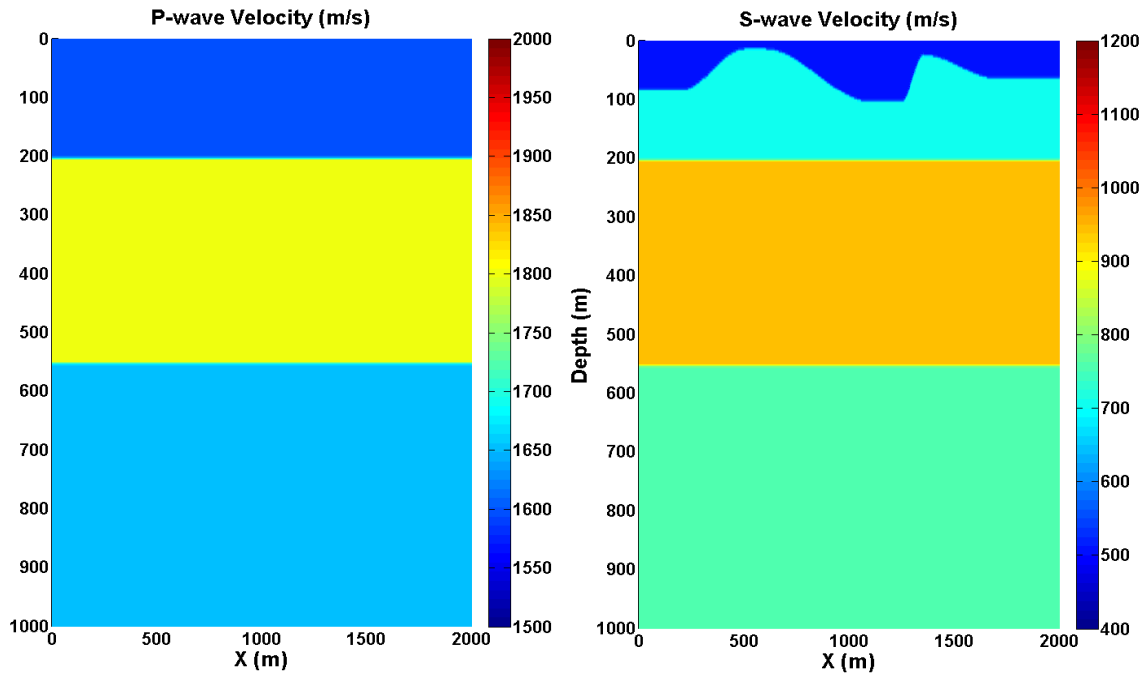


FIG. 2. P-wave (left) and S-wave (right) velocity models used for the elastic finite-difference modelling. Notice that there is no LVL in the  $V_p$  model and the LVL in the  $V_s$  model has been arbitrarily deformed.

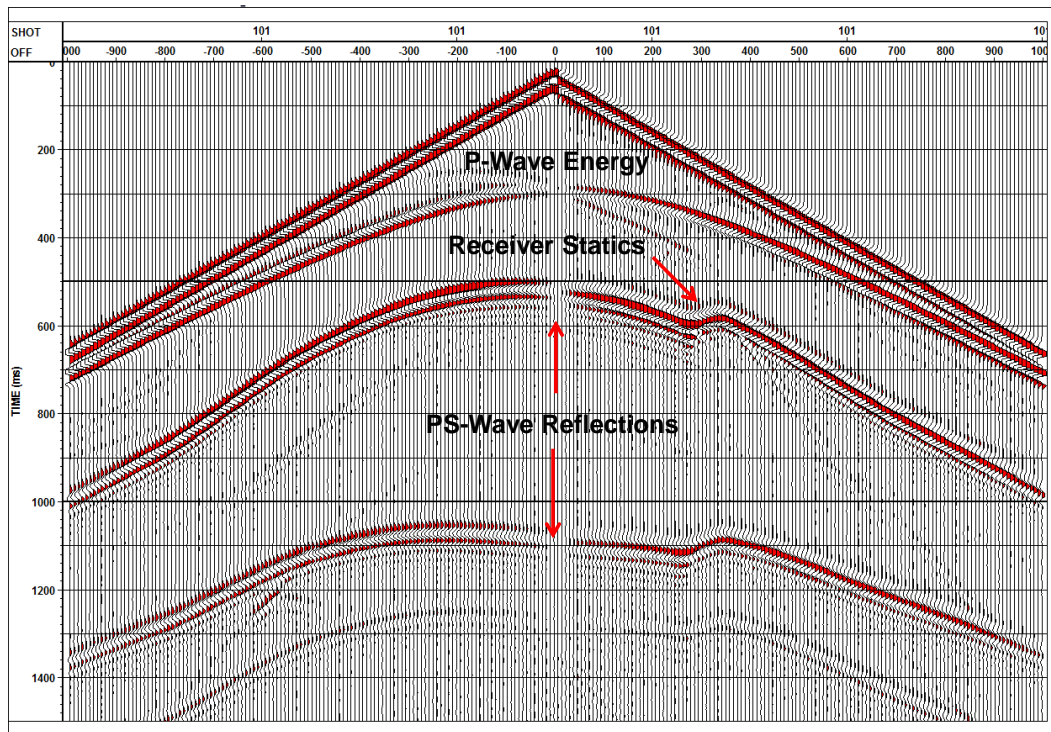


FIG. 3. Raw radial-component gather showing the most important features on the record.

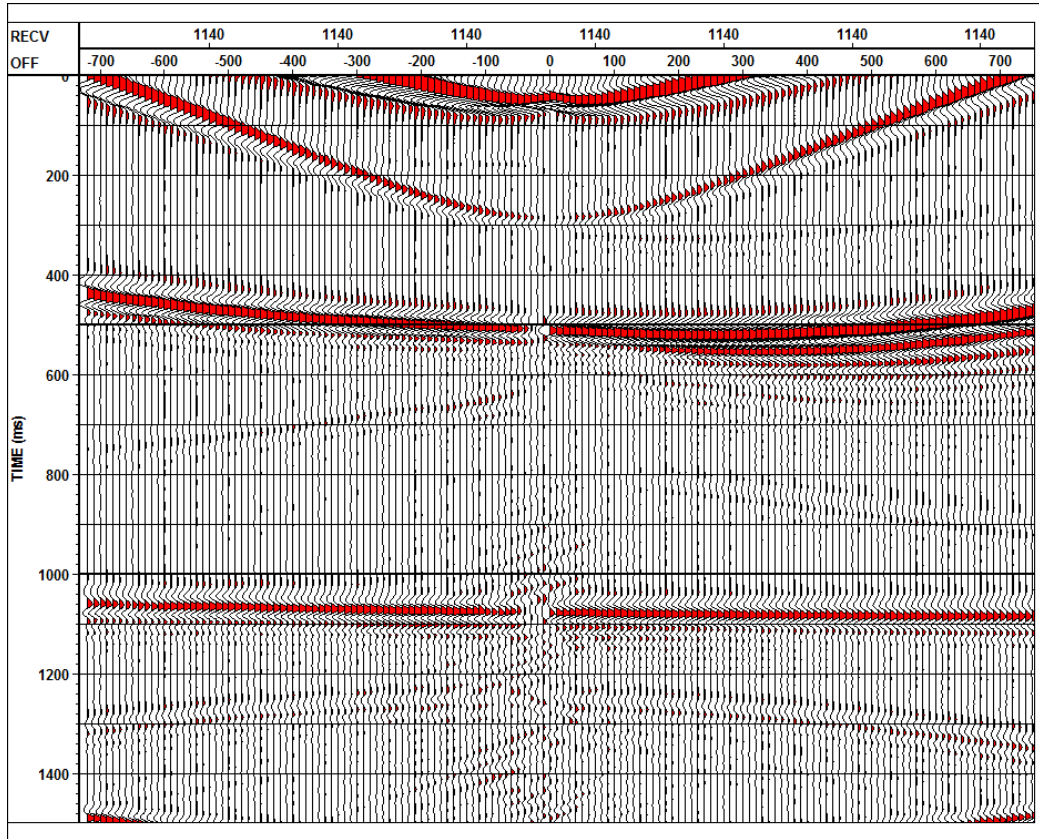


FIG. 4. Receiver gather at station 1140 sorted by signed offset.

the quasi-hyperbolic shape of the PS-reflection. Since both reflectors are known to be flat, any delay time other than the moveout of the reflection, must be due to S-wave statics.

A non-hyperbolic PS-NMO correction (Slotboom, 1990) was applied to the data to try to flatten the reflections. Figure 4 shows the receiver gather located at  $x=1140$  m corrected by PS-NMO. First, we can notice that there is an important residual moveout for the shallow reflector. However, the most important feature is that even for short and medium offsets there is a difference in the reflection times between traces at positive and negative offsets. For the deep reflector the residual moveout effect is less important but there is still a time difference between the reflection times for positive and negative offsets. This problem is an effect of the differences in the structure of the LVL at each side of the receiver.

### Interferometric raypath-consistent statics computation

The interferometric approach for solving static problems relies on the use of entire cross-correlation functions for shifting traces (Henley and Daley, 2009). These functions are computed after cross-correlating raw traces with pilot traces that have been "smoothed" for diminishing the traveltimes component due to the statics effect. Computation of the statics in the rayparameter domain is needed to account for changes in the structure and in the transmission angle through the LVL.

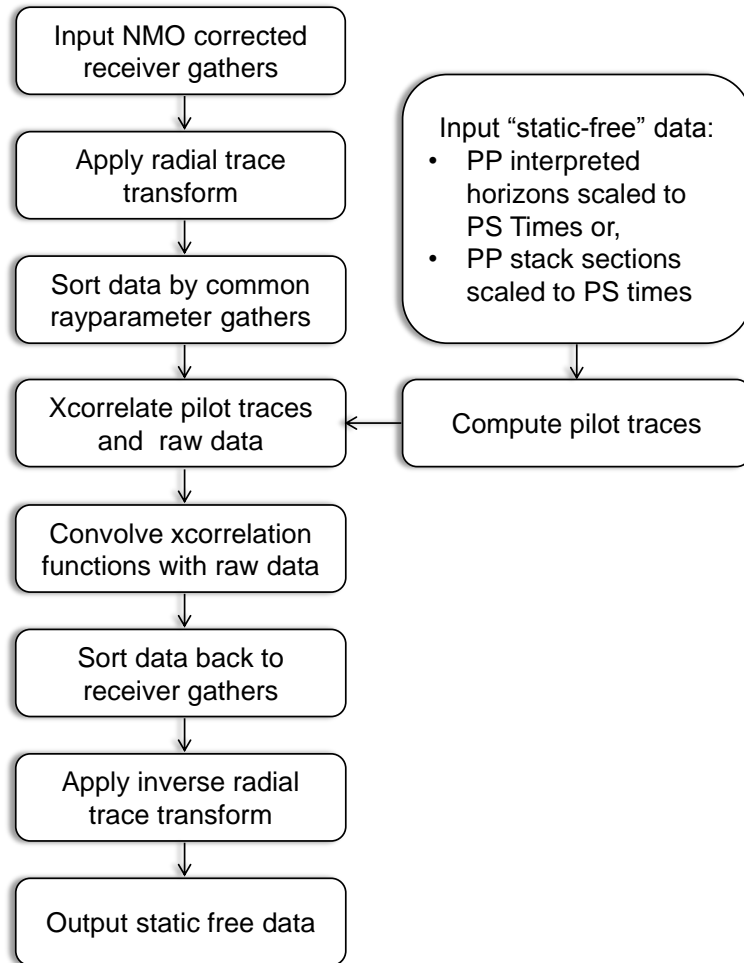


FIG. 5. Workflow followed for solving S-wave statics in the R-T domain using traveltime interferometry.

Since the radial-trace (R-T) transform has the effect of approximately simulating seismic data recorded along straight raypaths (Henley, 2000), NMO-corrected receiver gathers were transformed to the R-T domain to achieve the raypath consistency. An exponential gain function and polarity correction were applied to the traces before this process. The workflow used in this work is shown in Figure 5.

After sorting the data in receiver gathers and transforming them to the R-T domain, the data were gathered by common-rayparameter values. It is important to note that in this context the term "rayparameter" refers to the slope in the space-time (X-T) domain along which the R-T transform collects the amplitude values to create a radial trace. Figure 6 shows the rayparameter trace 500 m/s, for all the receiver stations. There, it is possible to see the structural effect of the LVL on the shape of the reflectors.

Since static problems are characterized for affecting the full length of the trace, a trim statics algorithm between 300 and 1300 ms was used for aligning the reflectors and computing the pilot traces. Additionally, a trace mixing filter using a wide lateral window (51

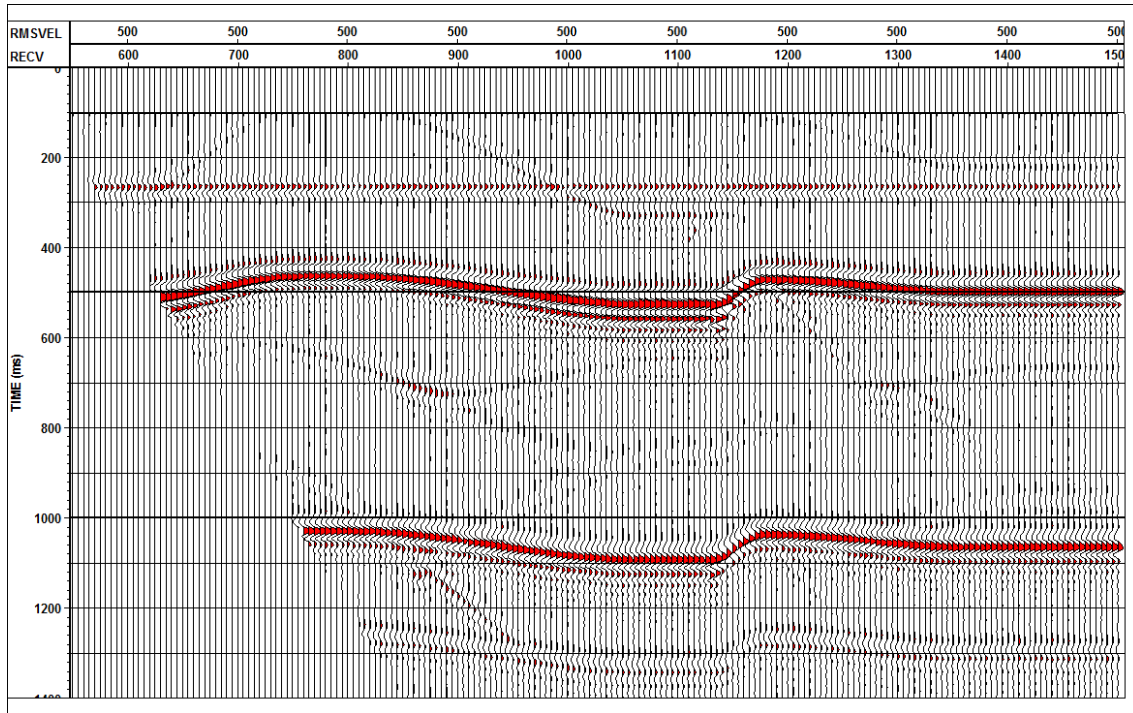


FIG. 6. Rayparameter gather 500 m/s.

traces) and a spectral whitening process were applied for improving coherency and frequency content respectively. Figure 7 shows the pilot gather for the rayparameter 500 m/s. Pilot gathers were computed for every rayparameter gather in the dataset.

Figure 8 shows the resulting traces after cross-correlating the rayparameter gathers with its pilot traces, for the 20 m/s (top) and 500 m/s (bottom) rayparameter values. There, it is possible to see how the cross-correlation functions have captured the delay times associated with the structure of the LVL. Furthermore, there is a slight difference between the delays associated with rayparameter 20 m/s, which is close to a vertical raypath, and rayparameter 500 m/s. Particularly, between receiver stations 1000 and 1150 it is very clear how the (bottom) cross-correlations have an additional delay of around 10 ms with respect to the (top) ones. It is important to note that the cross-correlation functions have been raised to the power of 5 in order to favor the largest peak and whiten the resulting traces (Henley, 2010).

Following the workflow, the cross-correlation functions are convolved with the raw traces to remove the captured delay times. Figure 9 shows the output of this process for the rayparameter gather 500 m/s. It is very clear how the reflections are perfectly aligned after the delay times caused by the statics were removed for the convolution process.

It is important to note that if the input to compute the cross-correlation functions is switched the resulting functions must be reversed before using them in the convolution step. Another option could be to replace the convolution operator by a cross-correlation

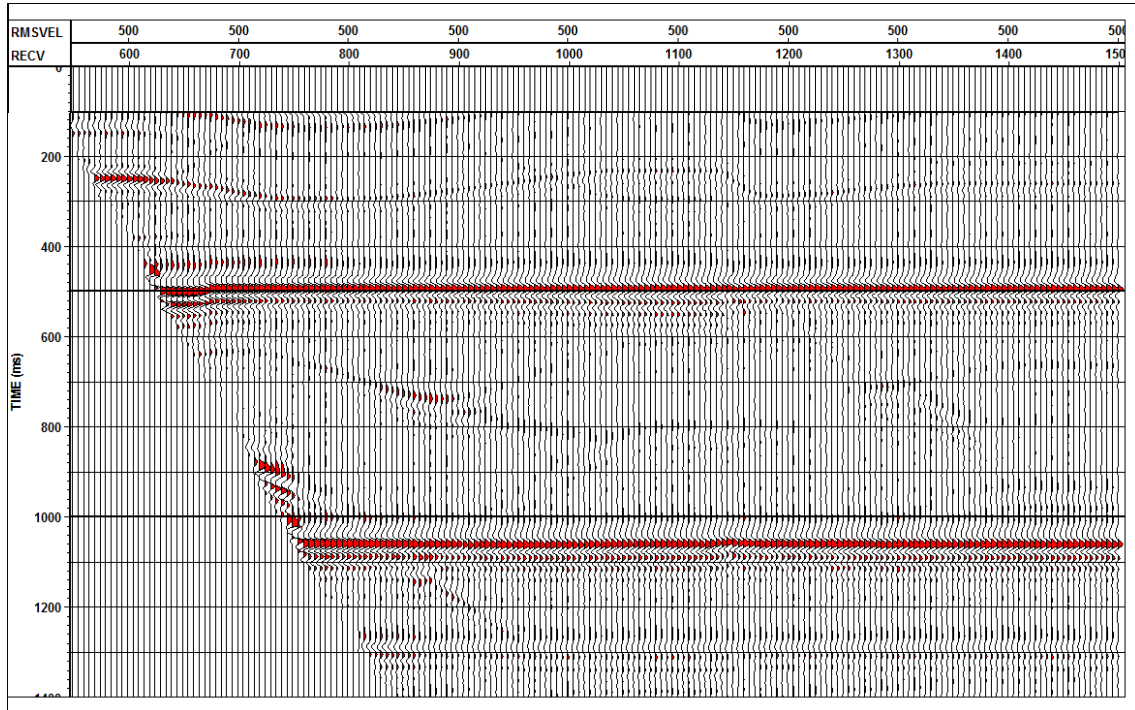


FIG. 7. Pilot gather (rayparameter 500 m/s) used for cross-correlation with the raw gathers.

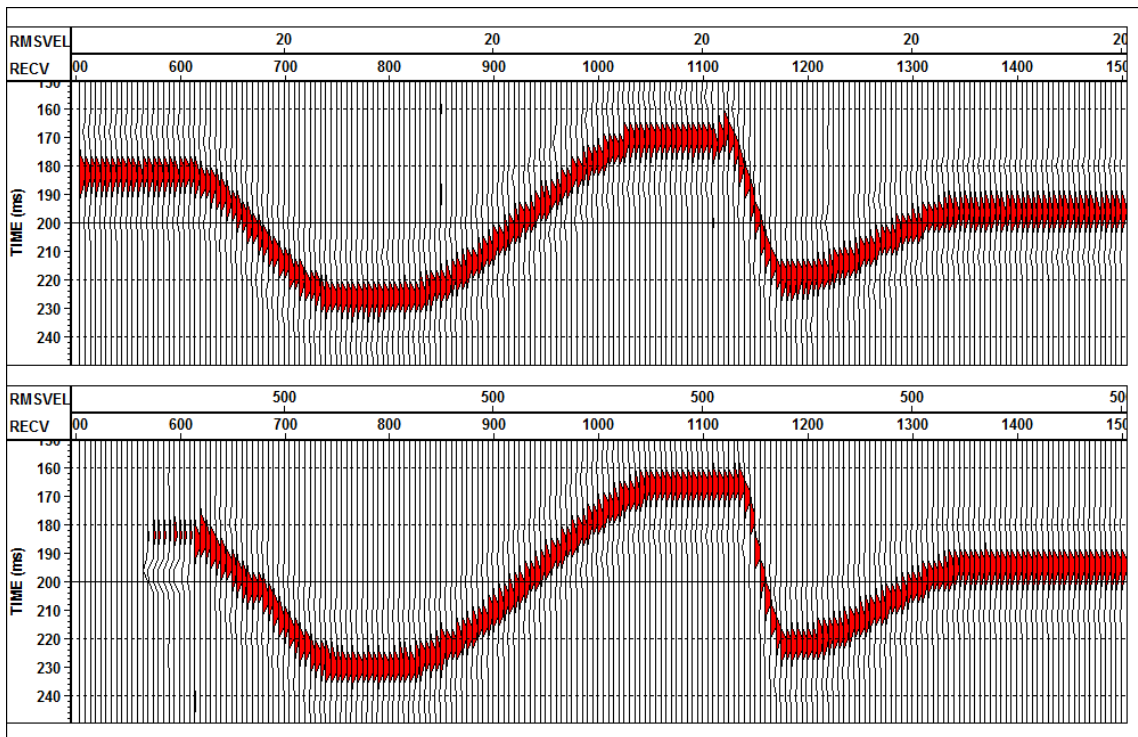


FIG. 8. Cross-correlation functions for the rayparameter 20 m/s (top) and 500 m/s (bottom)

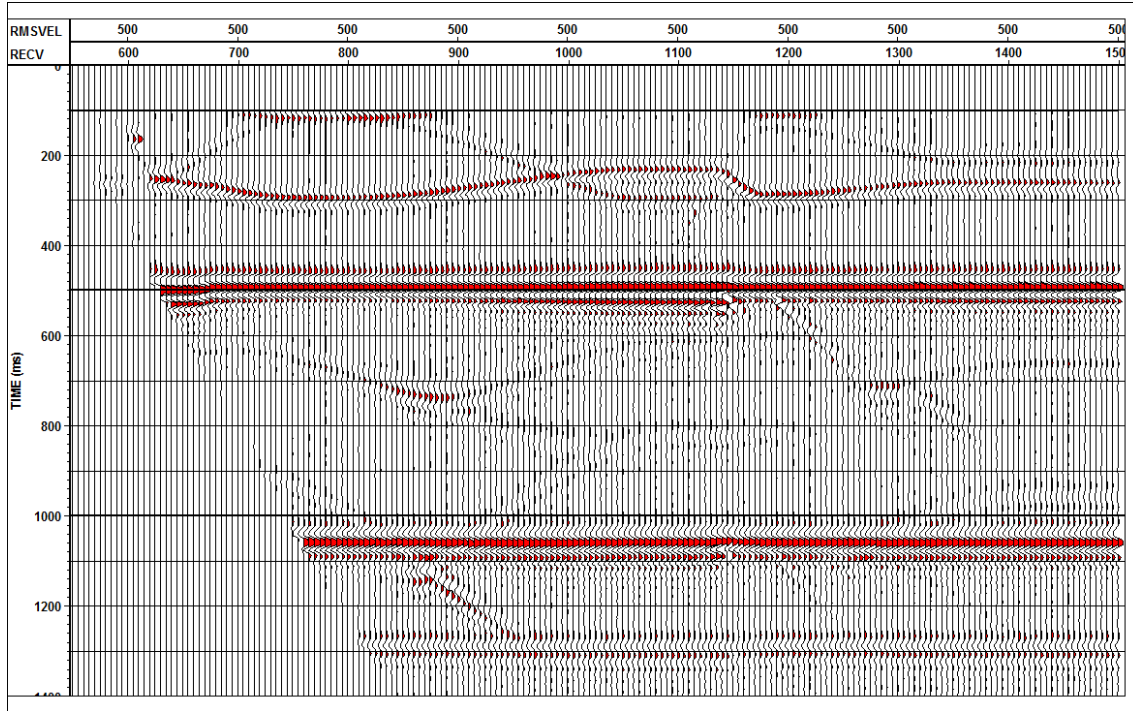


FIG. 9. Rayparameter gather 500 m/s after convolution with the cross-correlation functions.

operator, in which case there is no need to reverse the input functions.

In order to return the data to the X-T domain an inverse R-T transform was applied. In Figures 10 and 11 the CCP 1140 is shown, before and after statics corrections, respectively. It is very clear how after the application of the static corrections both reflectors show a very good alignment. The flatness achieved in Figure 11 assures a better stacking power than stacking reflections in Figure 10 which are deformed by the statics.

Finally, Figures 12 and 13 show the stacked sections with surface-consistent and raypath-consistent static corrections. For the surface-consistent solution the vertical traveltimes in the LVL were computed at each receiver location and then removed from the data. In Figure 12 it can be seen that the shallow reflector is not totally flat and the largest deviations are located on the parts of the sections where we know the LVL has some dip. The deep reflector shows a similar effect but in a lower magnitude. This difference must be due to the fact that the wavefield reflected from the deep horizon must have approached the base of the LVL with raypath angles closer to the vertical, making the surface-consistent solution suitable for removing the statics. However, for the shallow reflector there must be a wider range of transmission angles in the LVL. Hence, it can be concluded that the surface-consistent solution is not a good option when both shallow and deep reflectors need to be corrected.

On the other hand, both reflectors in Figure 13 show to be flat and coherent along the whole section. This allows us to conclude that under the presence of a structurally complex LVL computing the statics in the R-T domain effectively solved the problem of non-stationarity.

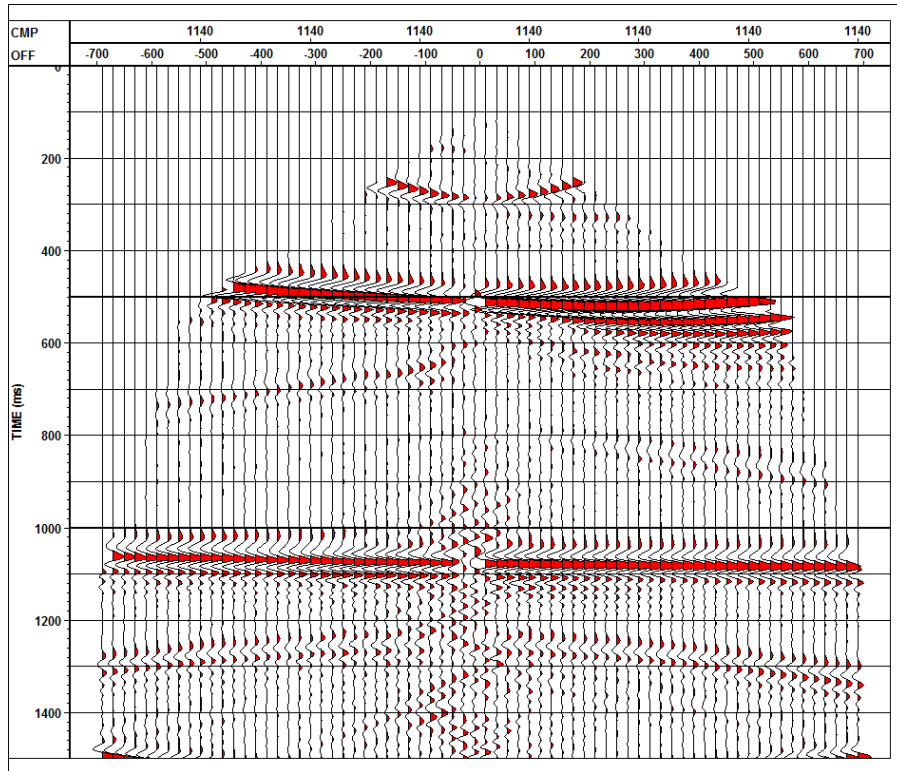


FIG. 10. CCP Gather 1140 before static corrections.

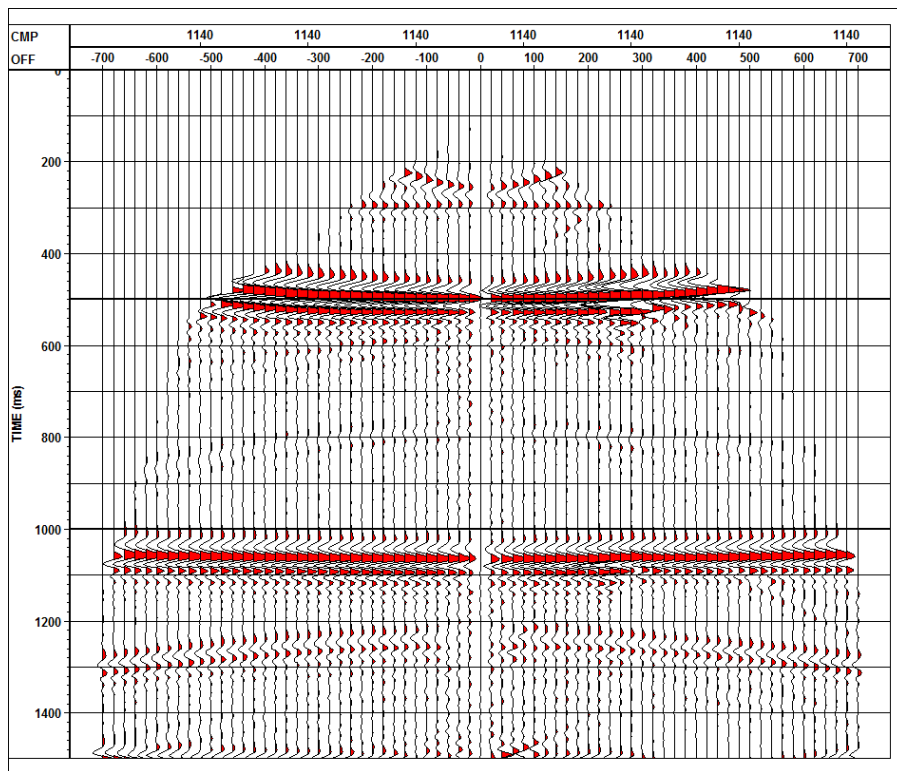


FIG. 11. CCP Gather 1140 after static corrections.

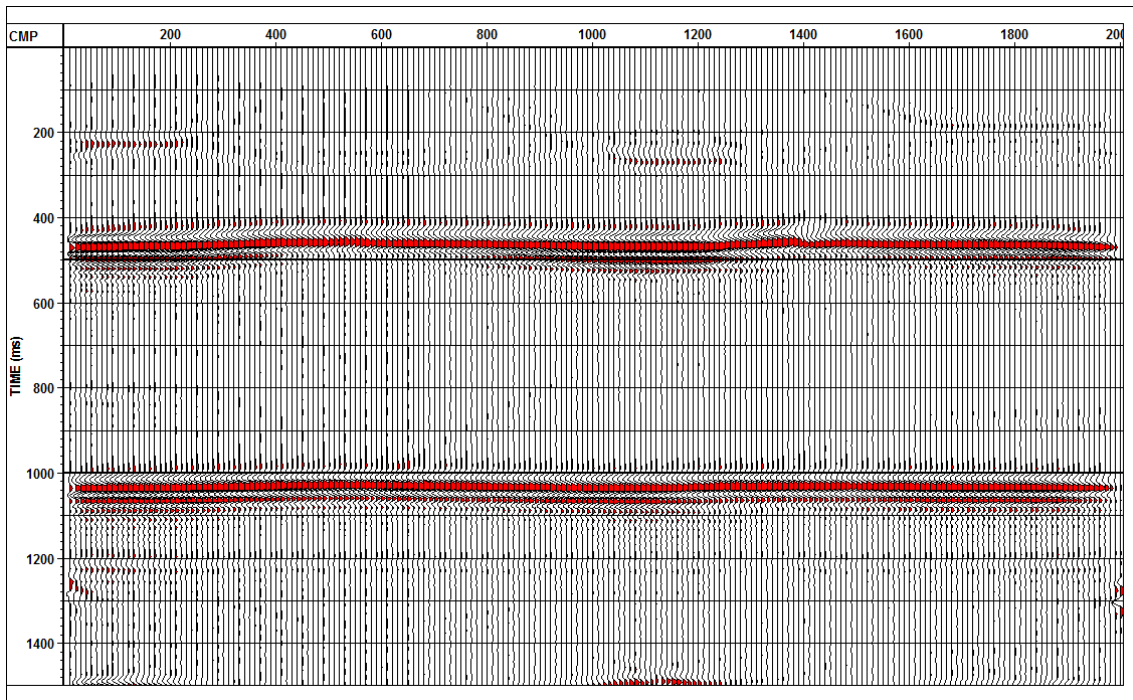


FIG. 12. CCP stack with surface-consistent static corrections.

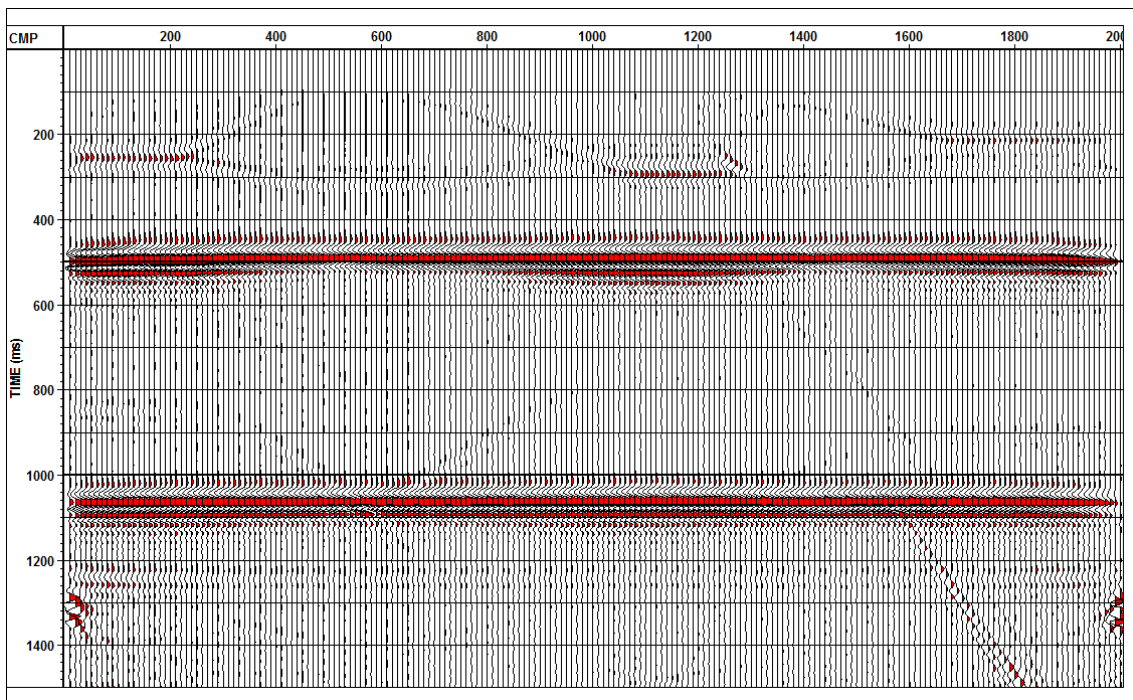


FIG. 13. CCP stack with raypath-consistent static corrections.

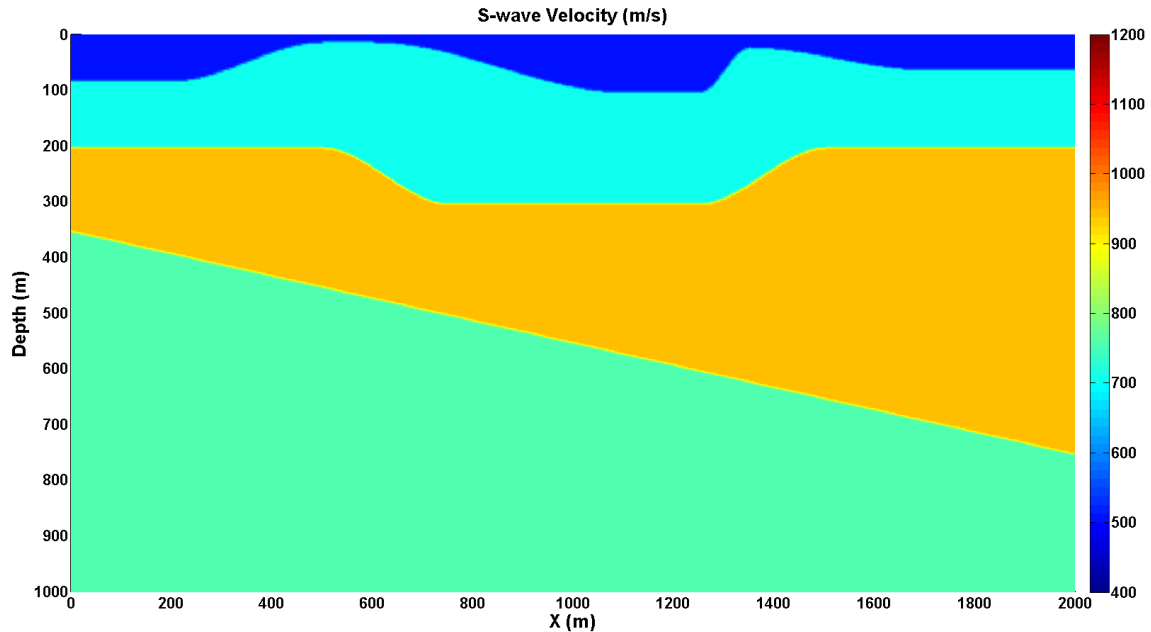


FIG. 14. S-wave velocity model used for computing synthetic data considering a structurally complex LVL and dipping reflectors.

### Structurally complex reflectors

It is important to note that forcing the rayparameter gathers to be flat was based on our knowledge about the geometry of the reflectors. When processing real data, this information can be given by interpreting the PP section. Horizons interpreted in PP time can be scaled to PS time and used for removing the structural component from the PS reflectors. The remaining time shifts must be due to the statics and they can be solved by forcing the reflector to be flat. After this process, the structural component can be added back to the data to get a "static-free" pilot trace.

Figure 14 shows the S-wave velocity model used for testing the interferometric raypath-consistent static solution proposed in this work, when reflectors have some structural complexity. It is expected that under this condition raypath dependency gets enhanced. This can be noted in Figure 15, where we can see that the surface-consistent solution was not able to remove the statics from either reflector. Particularly between CCP's 1200 to 1400, where the LVL has its larger dip, the right flank of the depressed feature in the shallow horizon can not be properly stacked. Moreover, the deep reflector is also deformed, and although it is known to have a constant dip it shows some deformation which is being imposed by the LVL.

These data were processed using the same workflow explained above. However, the process for building the pilot traces was slightly different. In this case the deep horizon was interpreted on the PP section and scaled to PS time. This horizon was used for flattening the rayparameter gather so the structure of that reflector was removed from the data. Then, the remaining shifts in the deep horizon were removed using a trim static process. After statics were removed, the horizon times were added back to create the pilot traces.

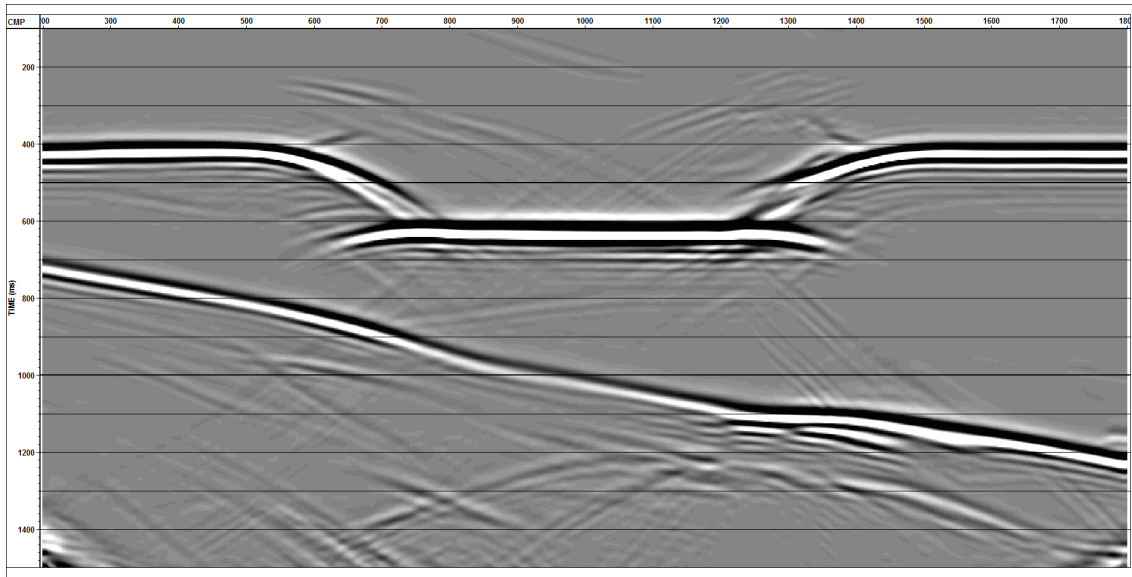


FIG. 15. PS-Stack section after using a surface-consistent solution for S-wave statics (Cova et al., 2013).

Figure 16 shows the resulting PS stack section for this case. As we can see the deformation caused by the statics were effectively removed from both reflectors. Both flanks of the depressed section on the shallow horizon are properly stacked and the deep reflector now shows a constant dip.

### Cross-correlation analysis

In order to understand the information retrieved by the cross-correlation functions we compared them with the traveltimes computed for a given range of raypath angles in the LVL, at a fixed receiver location. In Figure 17 (top) we can see the ray-tracing done for a receiver located just above a flat segment of the LVL. Figure 17 (middle) shows the traveltimes for each one of the raypaths displayed in the ray-tracing. For a flat LVL, Cova et al. (2013) show that the change of the traveltimes as a function of the raypath angles is in the form of  $t = (h/v)(1/\cos(\phi))$ , where  $h$  is the vertical thickness of the LVL,  $v$  is the velocity in the LVL and  $\phi$  is the raypath angle. In Cova et al. (2013), traveltimes computed using that relationship were compared with the ray-traced traveltimes showing a very good match. The important result here is that the cross-correlation functions showed at the bottom of Figure 17, display a similar trend. However, these cross-correlation functions were computed in the R-T domain, hence each trace represents a slope in X-T and not a direct raypath angle. A relationship between these two variables must be derived in order to relate the delay times captured by the cross-correlation functions in the R-T domain with a raypath angle.

In Figure 18 the same analysis is done but at a receiver location where the LVL is dipping. For this case we can still note that the new trend in the traveltimes imposed by the dip of the LVL is mimicked by the cross-correlation functions. Cova et al. (2013) show that

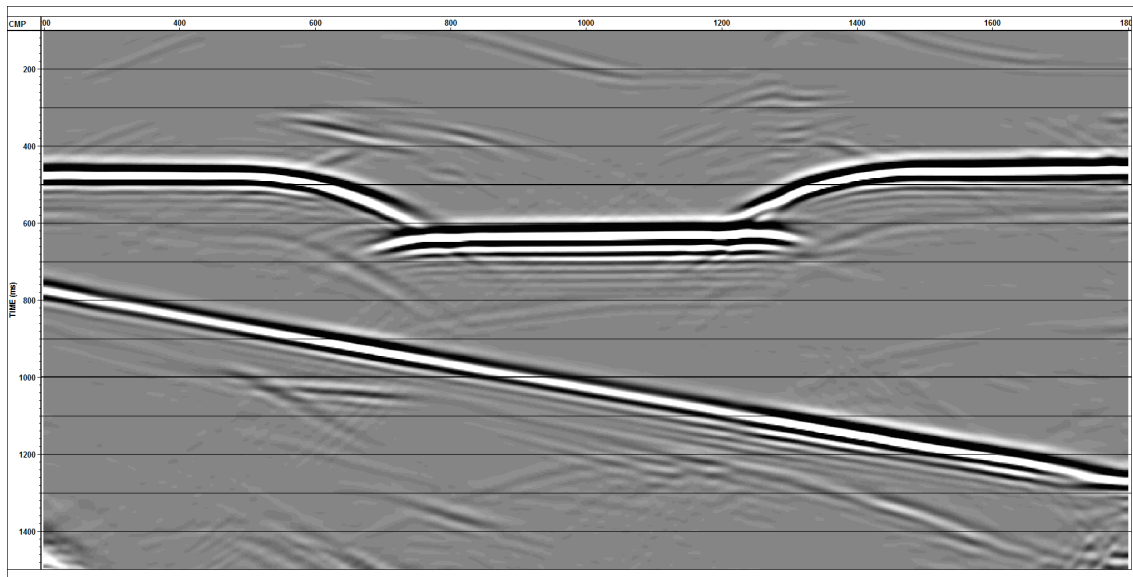


FIG. 16. PS-Stack section after using a raypath-consistent solution for S-wave statics (Cova et al., 2013).

for the case of a dipping LVL the traveltimes in the LVL as a function of the raypath angles can be computed as  $t = (h/v)(1/\cos(\phi + \theta))$ , where  $\theta$  is the dip at the base of the LVL. These results are the motivation for continuing this research heading toward the use of the cross-correlation delays for characterizing the thickness, dip and velocity of the LVL.

## CONCLUSIONS

In contrast to the refraction methods which rely on the time consuming task of identifying and picking first breaks, the reflection based approach shown here may be a better option for solving the static problems in a time efficient manner. Furthermore, the raypath consistent solution seems to be a very good approach when the LVL has some structural complexity that may lead to non-stationary statics. When not just the LVL is complex, but also the reflectors exhibit a structural component, the non-stationary character of the statics is enhanced and a raypath consistent solution is required to account for complex kinematics through the near surface.

Although the interferometric approach shown here does not require the computation of a velocity model to remove the static effect, as geoscientists it is our interest to retrieve a near-surface velocity model and obtain the details of the structure of the near-surface which is causing the statics. The early findings shown in this works indicate that the cross-correlation functions in the R-T domain are linked to the traveltimes in the near surface at different raypath angles. Moreover, the trend of the cross-correlation functions at a location where the LVL is known to be dipping follows very closely the trend of the traveltimes computed by ray-tracing. These observations along with the analysis done in Cova et al. (2013) are the starting points for a project focused on using the delay times captured by the cross-correlation functions in an inversion algorithm that may retrieve the information about the velocity and structure of the near surface.

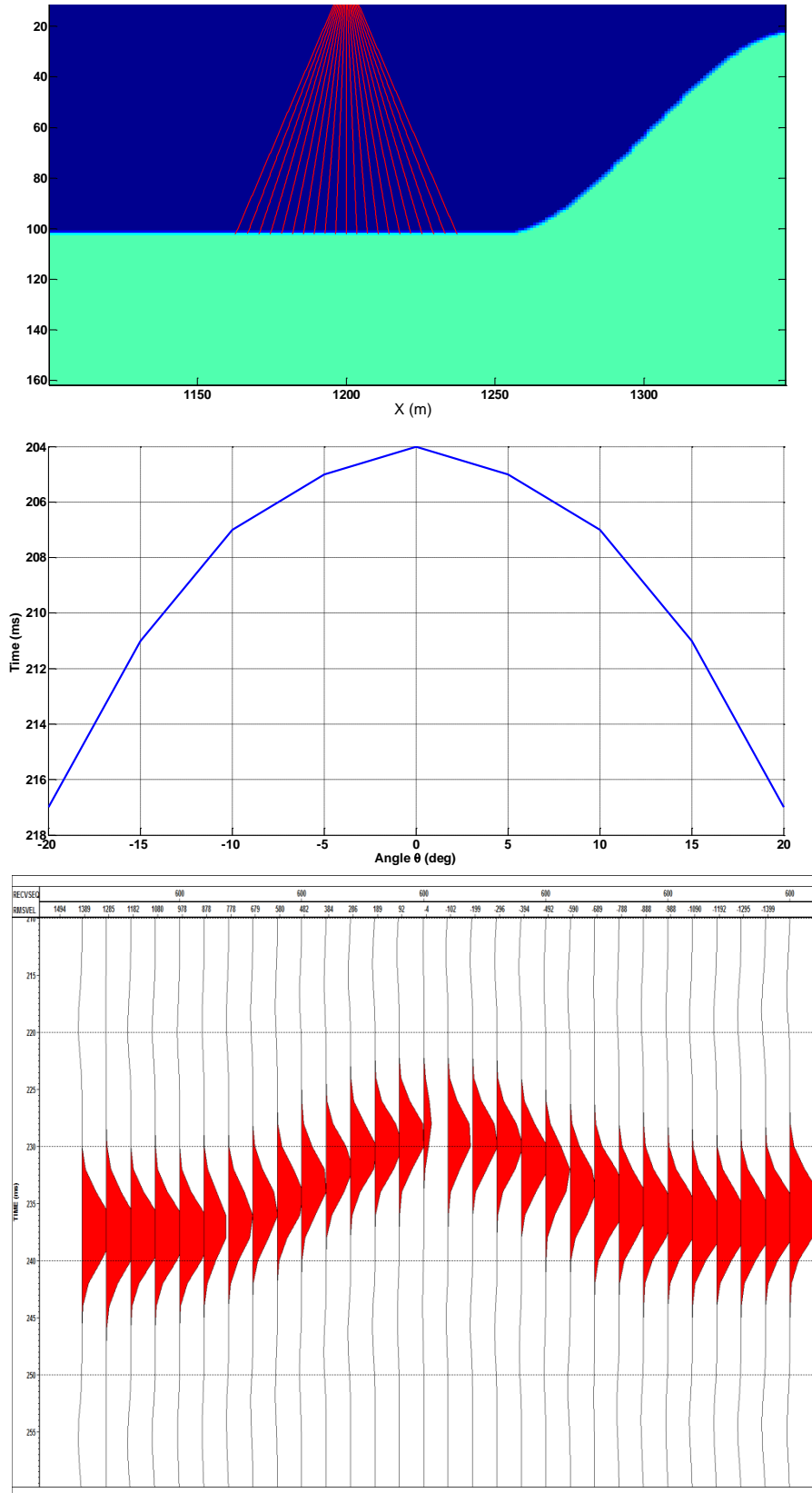


FIG. 17. (top) Ray-tracing at a flat segment of the LVL. (middle) Traveltimes computed as a function of the raypath angle. (bottom) Cross-correlation functions computed at the same receiver location.

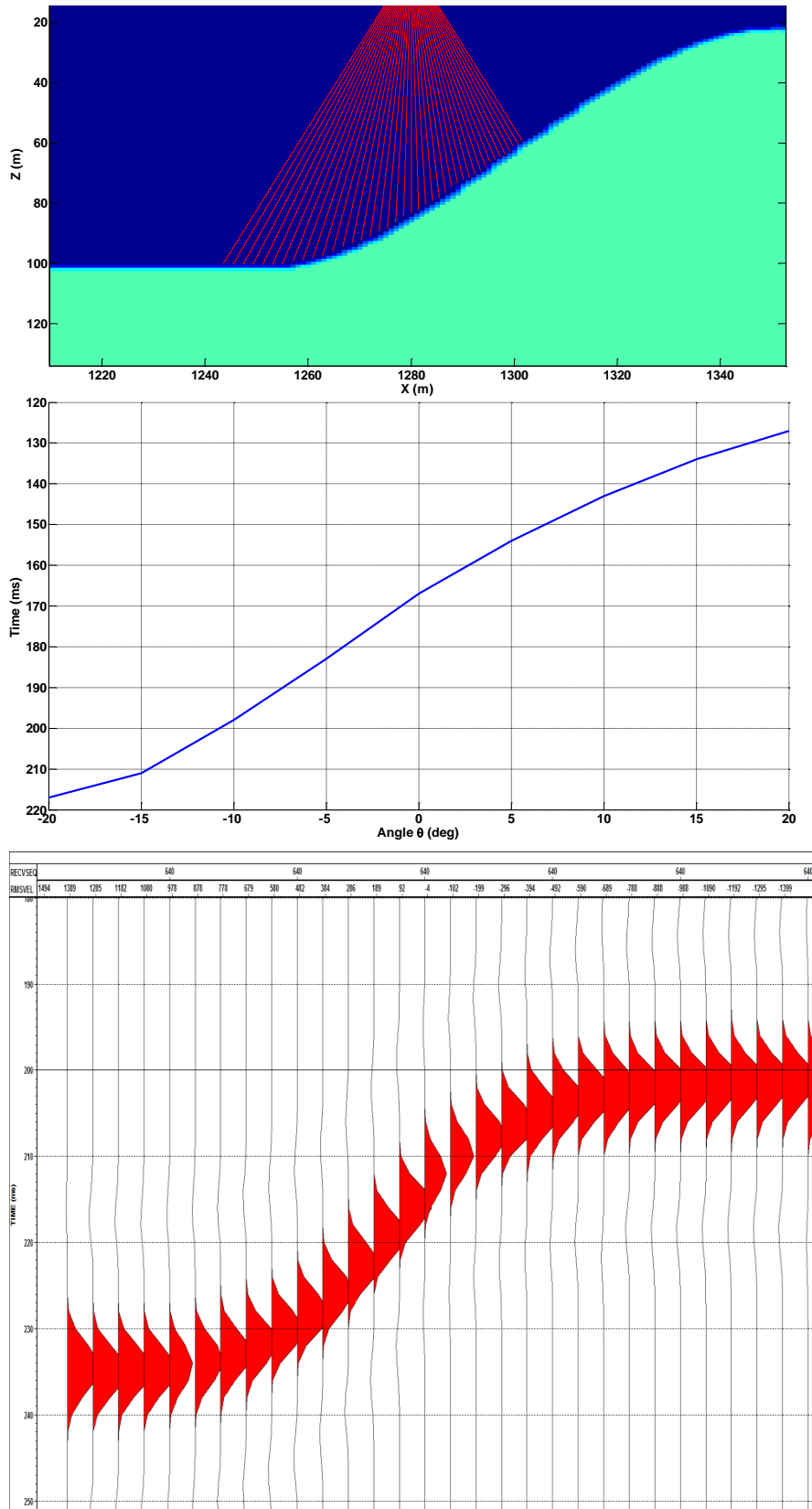


FIG. 18. (top) Ray-tracing at a dipping segment of the LVL. (middle) Traveltimes computed as a function of the raypath angle. (bottom) Cross-correlation functions computed at the same receiver location.

## ACKNOWLEDGEMENTS

The authors are thankful for the support provided by CREWES sponsors to this research.

## REFERENCES

- Bodet, L., van Wijk, K., Bitri, A., Abraham, O., Côte, P., Grandjean, G., and Leparoux, D., 2005, Surface-wave Inversion Limitations from Laser-Doppler Physical Modeling: *Journal of Environmental & Engineering Geophysics*, **10**, No. 2, 151–162.
- Cova, R., Henley, D., and Innanen, K., 2013, Non-stationary shear wave statics in the radial trace domain: CREWES Research Report, **25**.
- Dulaijan, K. A., 2008, Near-surface characterization using seismic refraction and surface-wave methods: M.Sc. thesis, Univ. of Calgary.
- Henley, D., 2000, More radial trace domain applications: CREWES Research Report, **12**, 21.1–21.14.
- Henley, D., 2010, Raypath interferometry for dummies: a processing guide: CREWES Research Report, **22**, 35.1–35.22.
- Henley, D., 2012, Interferometric application of static corrections: *GEOPHYSICS*, **77**, No. 1, Q1–Q13.
- Henley, D. C., and Daley, P. F., 2008, Applying interferometry to converted wave statics: CREWES Research Report, **20**, 36.1–36.16.
- Henley, D. C., and Daley, P. F., 2009, Hybrid interferometry: surface corrections for converted wave: CREWES Research Report, **21**, 32.1–32.18.
- Lin, C.-P., and Lin, C.-H., 2007, Effect of lateral heterogeneity on surface wave testing: Numerical simulations and a countermeasure: *Soil Dynamics and Earthquake Engineering*, **27**, No. 6, 541 – 552.
- Schafer, A. W., 1991, Converted-wave statics methods comparison: CREWES Research Report, **3**, 8.107–8.125.
- Slotboom, R. T., 1990, Converted wave (P-SV) moveout estimation: SEG Technical Program Expanded Abstracts, 1104–1106.